FEBS Letters 587 (2013) 562–568

journal homepage: www.FEBSLetters.org

Crystal structure of Cmr5 from *Pyrococcus furiosus* and its functional implications

Jeong-Hoh Park [1], Jiali Sun [1], Suk-Youl Park, Hyo-Jeong Hwang, Mi-Young Park, Minsang Shin, Jeong-Sun Kim *

Department of Chemistry and Institute of Basic Sciences, Chonnam National University, 300 Yongbong-dong, Buk-gu, Gwangju 500-757, Republic of Korea

ARTICLE INFO

Article history:
Received 5 November 2012
Revised 8 January 2013
Accepted 9 January 2013
Available online 28 January 2013

Edited by Stuart Ferguson

Keywords:
Cmr5
Clustered regularly interspaced short palindromic repeats
Crystal structure

ABSTRACT

The bacterial acquired immune system consists of clustered regularly interspaced short palindromic repeats (CRISPRs) and CRIPSR-associated (Cas) genes, which include Cas-module repeat-associated mysterious proteins (Cmr). The six Cmr proteins of *Pyrococcus furiosus* (pfCmr1–pfCmr6) form a Cmr effector complex that functions against exogenous nucleic acid. Among the Cmr proteins, the role of pfCmr5 and its involvement in the complex's cleavage activity have been obscure. The elucidated pfCmr5 structure has two inserted α-helices compared with the other trimeric Cmr5 structure. However, pfCmr5 exists as a monomeric protein both in the crystalline state and in solution. In vitro assays indicate that pfCmr5 interacts with pfCmr4. These structural and biophysical data might help in understanding the complicated and ill-characterized Cmr effector complex.

Structured summary of protein interactions:
pfCmr4 and **pfCmr5** bind by molecular sieving (View interaction)
pfCmr4 and **pfCmr4** bind by molecular sieving (View interaction)
pfCmr5 and **pfCmr4** bind by ion exchange chromatography (View interaction)

1. Introduction

In bacteria and archaea, clustered regularly interspaced short palindromic repeats (CRISPRs) and CRIPSR-associated (Cas) proteins confer heritable and adaptive immunity against incoming genetic elements [1–5]. Among the two characteristic sequences in the CRISPR locus, variable and conserved repeat sequences, the information about the heritable and adaptive immunity is stored in the variable sequences, which are derived from past encounters and can be added from new exogenous genes [1,3,6,7].

In *Pyrococcus furiosus*, small crRNAs and the repeat-associated mysterious proteins (RAMPs) module-containing Cas proteins (Cmr) form a Cmr effector complex, which cleaves complementary exogenous target RNAs at a fixed distance from the 3′-end of the integral crRNAs. The isolated Cmr effector complex from the crude cell fraction of *P. furiosus* has been shown to contain six Cmr proteins (pfCmr1–pfCmr6). However, the elimination of pfCmr5 in the recombined effector complex leads to no observable effect on the cleavage activity against added RNA [8]. The Cmr effector complex in *Sulfolobus solfataricus* has also been confirmed to have six proteins (ssCmr1–ssCmr6). Furthermore, the complex includes another protein, ssCmr7 [9]. These data invoke questions concerning the composition of Cmr proteins and their roles in the effector complex.

Detailed information on the Cmr5 protein has been obtained from the recent crystal structure of Cmr5 from *Thermus thermophilus* HB8 (ttCmr5). The protein forms a single globular structure of six α-helices. Seven hydrophobic residues from the two neighboring molecules form a hydrophobic interaction at the interfaces, which has been suggested as a main force facilitating the assembly of a trimeric ttCmr3 structure. Furthermore, its molecular size in solution is close to the trimeric protein. In addition, ttCmr5 has been suggested to be a nucleic acid-binding protein based on the

Abbreviations: afCmr5, Cmr5 from *Archaeoglobus fulgidus*; ASU, asymmetric unit; Cas, CRIPSR-associated gene; Cmr, Cas-module RAMP; CRISPR, clustered regularly interspaced short palindromic repeats; M.W., molecular weight; PCR, polymerase chain reaction; PDB, Protein Data Bank; pI, isoelectric point; pfCmr5, Cmr5 from *P. furiosus*; RAMP, repeat-associated mysterious proteins; rmsd, root-mean-square deviation; SEC, size exclusion chromatography; SSRF, Shanghai Synchrotron Radiation Facility; TEV, tobacco etch virus; ttCmr5, Cmr5 from *Thermus thermophilus* HB8

* Corresponding author. Address: Department of Chemistry, College of Natural Science, Chonnam National University, 300 Yongbong-dong, Buk-gu, Gwangju 500-757, Republic of Korea. Fax: +82 62 530 3389.
E-mail address: jsunkim@chonnam.ac.kr (J.-S. Kim).

[1] These authors contributed equally to this work.

0014-5793/$36.00
http://dx.doi.org/10.1016/j.febslet.2013.01.029

Table 1
Data collection and refinement statistics.

Parameters	pfCmr5
Synchrotron	BL17U1, SSRF
Wavelength (Å)	0.9762
Space group	$P4_32_12$
Cell parameters	$a = b = 53.94$ Å, $c = 235.99$ Å, $\alpha = \beta = \gamma = 90°$
Resolution (Å)	50.0–2.0 (2.03–2.0)
Completeness (%)	93.2 (85.4)
R_{sym}[a] (%)	5.7 (46.5)
Reflections, total/unique	102, 154/23 080
R_{factor}[b] (%)/R_{free}[c] (%)	20.8/26.0
No. of atoms, protein/water	2, 423/183
rmsds, bonds Å/angles o	0.002/0.69
Geometry (%)	
Favored	99.65
Allowed	0.35
Outliers	0

Values in parentheses are for the highest-resolution shell.
rmsds: root-mean-square deviations.
[a] $R_{sym} = \sum_{hkl}\sum_j |I_j - \langle I\rangle| / \sum_{hkl}\sum_j I_j$, where $\langle I\rangle$ is the mean intensity of reflection *hkl*.
[b] $R_{factor} = \sum_{hkl} ||Fobs| - |Fcalc|| / \sum_{hkl} |Fobs|$, where Fobs and Fcalc are, respectively, the observed and calculated structure factor amplitudes for the reflections hkl included in the refinement.
[c] R_{free} is the same as R_{factor} but is calculated over a randomly selected fraction (8%) of the reflection data not included in the refinement.

conserved RAMP module structure and localized basic patch at the subunit interface [10]. On the other hand, the crystal structure of Cmr5 from *Archaeoglobus fulgidus* (afCmr5), which has been deposited in the Protein Data Bank (PDB) and publicly released (PDB ID 2oeb at http://www.rcsb.org/pdb), contains a single molecule in the asymmetric unit (ASU). However, a trimeric molecule cannot be generated by applying the crystallographic H32 symmetry. These data indicate that the biophysical properties of Cmr5 and its role in the formation of the effector complex are still controversial and should be investigated.

We elucidated the crystal structure of pfCmr5. A comparison with ttCmr5 revealed the insertion of two α-helices in the middle of the aligned sequence. Two molecules in the ASU cannot generate a trimeric structure that has been shown in ttCmr5. Furthermore, pfCmr5 behaved as a monomer in solution. Our in vitro binding assays exhibited the presence of a direct interaction between the pfCmr5 and pfCmr4 proteins.

2. Materials and methods

2.1. Cloning, expression, and purification of pfCmr5 and pfCmr4

The *P. furiosus* genes coding for pfCmr5 (Met1-Ser169, M.W. 19.7 kDa) and pfCmr4 (Met1-Lys295, M.W. 32.6 kDa) were

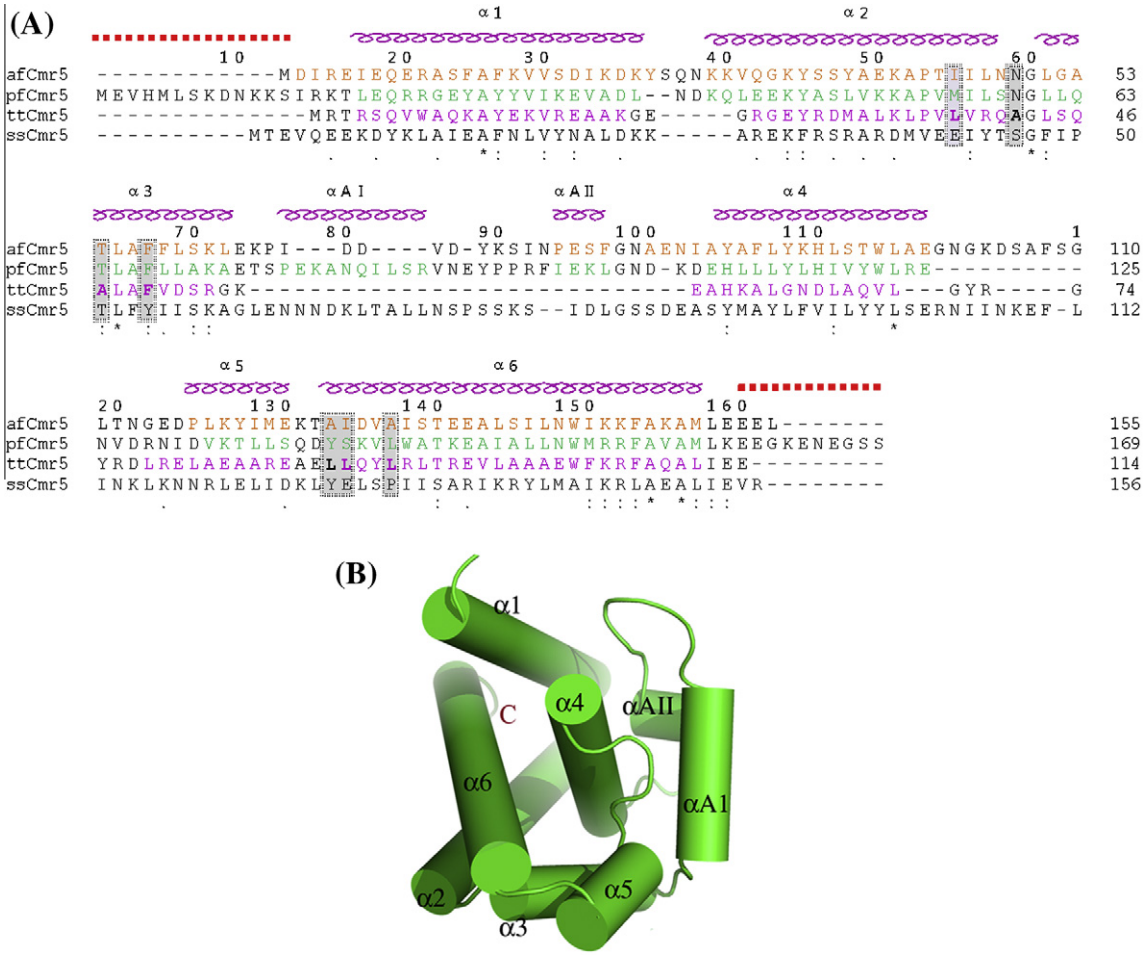

Fig. 1. The overall features of pfCmr5. (A) Structure-based sequence alignment of Cmr5s. The amino acid sequences are shown for Cmr5 from *P. furiosus* (pfCmr5), Cmr5 from *T. thermophilus* HB8 (ttCmr5), Cmr5 from *A. fulgidus* (afCmr5), and Cmr5 from *S. solfataricus* (ssCmr5). The coils (α) stand for the α-helix. The numbering scheme follows the amino acid sequence of pfCmr5. The continuous red-dotted lines above the aligned sequences display the extreme N-terminal and C-terminal regions that were not traced in the present structure. Identical residues are marked by "∗". Conserved residues are indicated by ":" or ".", respectively. The residues in the α-helices are colored. The residues forming hydrophobic interactions at the interfaces of two subunits are indicated by bold in the dotted boxes of grey background. The sequence alignment was prepared using the ClustalW2 program of the European Bioinformatics Institute and based on primary amino acid sequences [19]. (B) The overall shape of pfCmr5. The α-helices are represented as cylinders.

amplified by polymerase chain reaction (PCR) using *P. furiosus* chromosomal DNA as a template and primers designed for Ligation-Independent Cloning [11]. The amplified PCR products were prepared for vector insertion by purification and treatment with T4 DNA polymerase (New England Biolabs, Beverley, MA) in the presence of 1 mM dTTP. The prepared inserts were annealed into a derivative of pET21a (Novagen, Madison, WI) that expressed the cloned gene fused with an N-terminal 6-His-Tobacco etch virus (TEV) cleavage sequence. The expression constructs were transformed into a *Escherichia coli* BL21(DE3)star strain, which was grown in 1 l of LB medium containing ampicillin (100 μg/ml) at 310 K. After induction via the addition of 1.0 mM IPTG, the culture medium was maintained for an additional 8 h at 310 K. The cells were harvested by centrifugation at 5000×*g* at 277 K. The cell pellet was resuspended in buffer A (20 mM Tris–HCl at pH 7.5 and 500 mM NaCl) and then disrupted by ultrasonication. The cell debris was removed by centrifugation at 11 000×*g* for 1 h. The fusion protein was purified using a 5-ml HisTrap chelating column (GE healthcare, Uppsala, Sweden). The column was extensively washed with buffer A, and the bound protein was eluted with a linear gradient of 0–500 mM imidazole in buffer A. After cleavage with the recombinant TEV protease and removal of salts by dialysis against buffer B (20 mM Tris–HCl at pH 7.5), the pfCmr5 protein was purified using a 5 ml HiTrapSP cation exchange column (GE healthcare, Uppsala, Sweden). The column was extensively washed with buffer B and the bound pfCmr5 was then eluted with approximately 150 mM NaCl in buffer B. On the other hand, pfCmr4 was purified using a 5-ml HiTrapQ anion exchange column (GE healthcare, Uppsala, Sweden) and the bound pfCmr4 was then eluted with approximately 400 mM NaCl in buffer B.

2.2. Crystallization, data collection, and structure determination of *pfCmr5*

For crystallization, the purified pfCmr5 protein was concentrated to 12 mg/ml in a buffer consisting of 20 mM Tris–HCl at pH 7.5 and 300 mM NaCl. The pfCmr5 crystals suitable for diffraction experiments were obtained within 5 days using a hanging-drop vapor-diffusion method at 22 °C by mixing 1 μl each of protein solution and reservoir solutions and equilibrating against 200 μl of reservoir solution, consisting of 20% (w/v) Polyethylene Glycol 3350, 0.1 M Bis-Tris–HCl at pH 7.5, and 0.2 M Magnesium Chloride. The diffraction data for the pfCmr5 crystal were collected at the BL17U1 beamline of the Shanghai Synchrotron Radiation Facility (SSRF) in China. The data were then indexed, integrated, and scaled with the HKL-2000 suite [12]. The crystal structure of

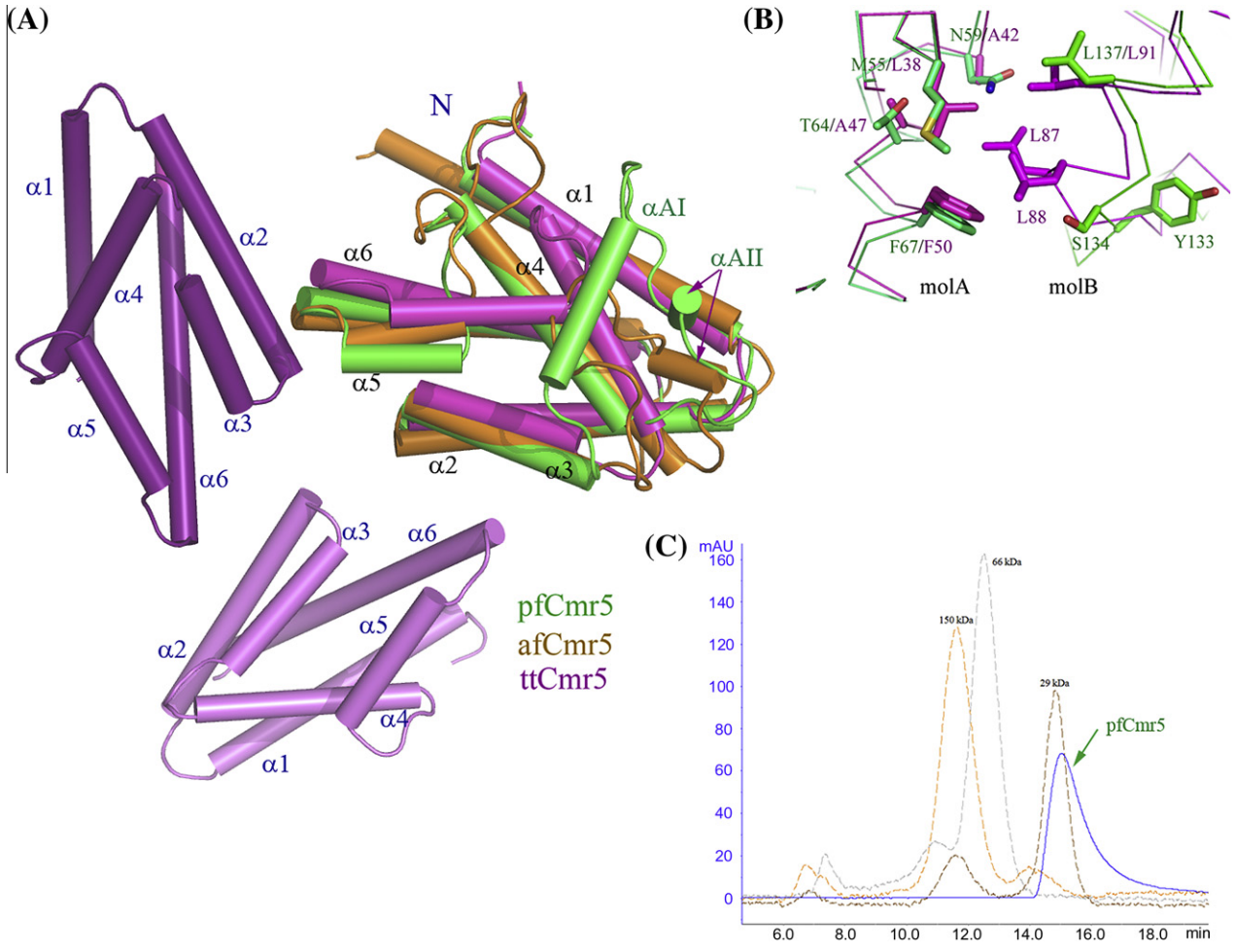

Fig. 2. A comparison of three revealed Cmr5 structures. (A) Three superposed Cmr5 structures are displayed and labeled with discerned colors. The afCmr5 in orange and pfCmr5 in green were superposed on the trimeric ttCmr5 in magenta. The common α-helices of all three Cmr5s are labeled in black. The additional αAI-helix in pfCmr5 and another αAII-helix in pfCmr5 and afCmr5 are labeled in green. (B) A comparison at the subunit interface of the trimeric ttCmr5 with pfCmr5. The non-polar residues from two molecules (molA and molB) that mediate the oligomeric structure in ttCmr5 and corresponding residues in pfCmr5 are displayed with stick models and differentiated by colors. The colors and labels used are the same as described in (A). (C) Analysis of the oligomeric state of pfCmr5 by SEC. The protein standards used are alcohol dehydrogenase (150 kDa), human serum albumin (66 kDa), and carbonic anhydrase (29 kDa). The profile for the injected pfCmr5 is drawn with a blue line.

pfCmr5 was solved at 2.0 Å resolution by the molecular replacement program Phaser-1.3 [13] using the afCmr5 structure (PDB ID 2oeb) as a search model. Further model building was performed manually using the programs WinCoot [14] and O [15]. Refinement was performed with PHENIX [16] and CNS [17]. The statistics for the collected data and refinement are summarized in Table 1. The quality of the model was analyzed with WinCoot [14] and MolProbity [18]. Figures for the ribbon diagram and ball-and-stick model were prepared using the PyMol Molecular graphics program (Delano Scientific).

2.3. Size-exclusion chromatography (SEC) analysis

The SEC analyses for the purified pfCmr5, pfCmr4, and the mixture of pfCmr4 and pfCmr5 were performed with an AKTA Explorer chromatography system using a Superose 12 size-exclusion column (10 × 300 mm, GE healthcare, Sweden) in a buffer consisting of 20 mM Tris–HCl at pH 7.5 and 100 mM NaCl at a flow rate of 0.5 ml/min. The chromatograms were obtained by monitoring the absorbance at 280 nm. A set of molecular mass standard markers (Sigma, USA) ranging from 29 to 150 kDa was used.

2.4. Data deposition

The coordinates and structure factors of pfCmr5 were deposited in the Protein Data Bank under the accession number 4gkf.

3. Results and discussion

3.1. Overall feature of pfCmr5

The pfCmr5 protein comprises 169 amino acids with a calculated theoretical molecular weight of approximately 20 kDa and an isoelectric point (pI) of 8.61. The crystal structure of the recombinant pfCmr5 was solved by molecular replacement and refined to a resolution of 2.0 Å. In the refined structure, five Gly residues from the expression construct, thirteen (Glu2–Ile14) at the N-terminus, and nine (Glu161–Ser169) at the C-terminus were disordered (red-dotted line in Fig. 1A). An analysis of the modeled residues by WinCoot [14] and MolProbity [18] indicated that they are located in valid regions of the Ramachandran plot (Table 1).

The traced 146 amino acids of pfCmr5 form eight α-helices, which comprise a single α-helical bundle structure (Fig. 1B). This single globular structure is mainly formed by the hydrophobic interaction between the central α4-helix and the seven surrounding α-helices. In addition to these hydrophobic interactions, polar interactions were observed. For example, the hydroxyl group of Tyr45 on the α2-helix interacts with the side chain of His110 on the α4-helix, which is connected to the side chain of Glu32 on the α1-helix through a water molecule. The side chain of Tyr108 on the α4-helix also interacts with Asn80 on the αAII-helix through another water molecule.

3.2. Structural comparison of pfCmr5 with other Cmr5 structures

The pfCmr5 has approximately 25% and 35% sequence identity with ttCmr5 and afCmr5 among the aligned 110 amino acids, respectively. The relatively well-conserved residues are located on the three α-helices, α2, α3, and α6 (Fig. 1A). These three α-helices are involved in assembling the trimeric ttCmr5 structure (Fig. 2A). The other three α-helices, α1, α4, and α5, are oriented towards the solvent at the opposite site to the trimeric axis in ttCmr5 (Fig. 2A) (10).

Three homologous proteins share a close structural similarity (Fig. 2A), which is indicated by small values of root-mean-square-deviations (rmsds) such as 1.5 and 1.4 Å among the compared 100 Cα atoms. However, a closer look reveals several differences on the superposed structures. The pfCmr5 has additional regions comprising approximately 10 amino acids at both the extreme N- and the C-terminus, which includes a number of charged

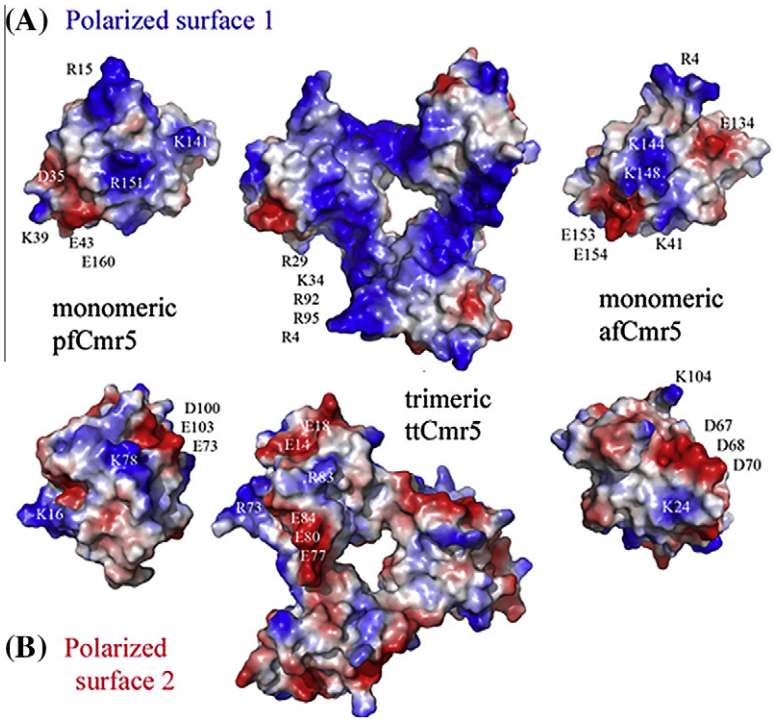

Fig. 3. Surface potential map of Cmr5. (A) Positively polarized surface 1. The positively charged surfaces are colored in blue and red, respectively. The residues of the polarizing surfaces are indicated. The monomeric pfCmr5 and afCmr5 molecules are oriented in the same direction of the left-upper monomer of trimeric ttCmr5 molecule. (B) Negatively polarized surface 2 that is located on the opposite site to (A). This figure was obtained by 180° rotation of (A).

residues. However, they are disordered in the present structure (red-dotted lines in Fig. 1A) and are not conserved in both afCmr5 and ttCmr5. Therefore, their roles in pfCmr5 might be negligible or be restrained.

The most remarkable difference can be found in the middle of the structure-based aligned sequences. Upon comparison with ttCmr5, the pfCmr5 has approximately 30 inserted residues between the α3- and α4-helices (Fig. 1A), compared with ttCmr5. They form two α-helices of a short αAI and a three-turn αAII. The afCmr5 has also a 20 amino-acid insertion at the corresponding region, which forms a short αAII-helix and a long flexible loop (Fig. 2A). These inserted regions in both Cmr proteins are located at the opposite site to the threefold axis of the superposed ttCmr structure (Fig. 2A), implying that it may not be related to oligomerization.

The third difference is found in their oligomeric states. The ttCmr5 protein has been reported to form a trimeric structure by the interaction of three α-helices (α2, α3, and α6) (Fig. 2A) [10]. More specifically, a hydrophobic interaction is formed at the interfaces of two molecules among the seven non-polar residues (Leu38, Ala42, Phe50, and Al47 from one molecule and Leu87, Leu88, and Leu91 from another molecule) (bold letters in Figs. 1A and 2B) on these three α-helices [10]. However, afCmr5 does not appear to form a trimeric structure in the reported crystalline state, nor does pfCmr5. To characterize the oligomeric state of pfCmr5 in solution, we performed SEC, which exhibited a single peak that eluted immediately after the referenced carbonic anhydrase (29 kDa) (Fig. 2C) and strongly indicated that 20-kDa pfCmr5 behaves as a monomeric protein in solution. At the primary sequence level, seven non-polar residues are not conserved and replaced with hydrophilic and bulky residues both in afCmr5 and pfCmr5 (residues in the dotted boxes in Fig. 1A). At the structural level, the main-chain atoms on the loop between the α2 and α3 helices of pfCmr5 are not well-superposed on those of ttCmr5 and the orientations of Tyr133 and Ser134 are located opposite of the hydrophobic pocket (Fig. 2B), implicating that no hydrophobic interaction might be formed here. These sequential and structural features suggest that a tight hydrophobic interaction that

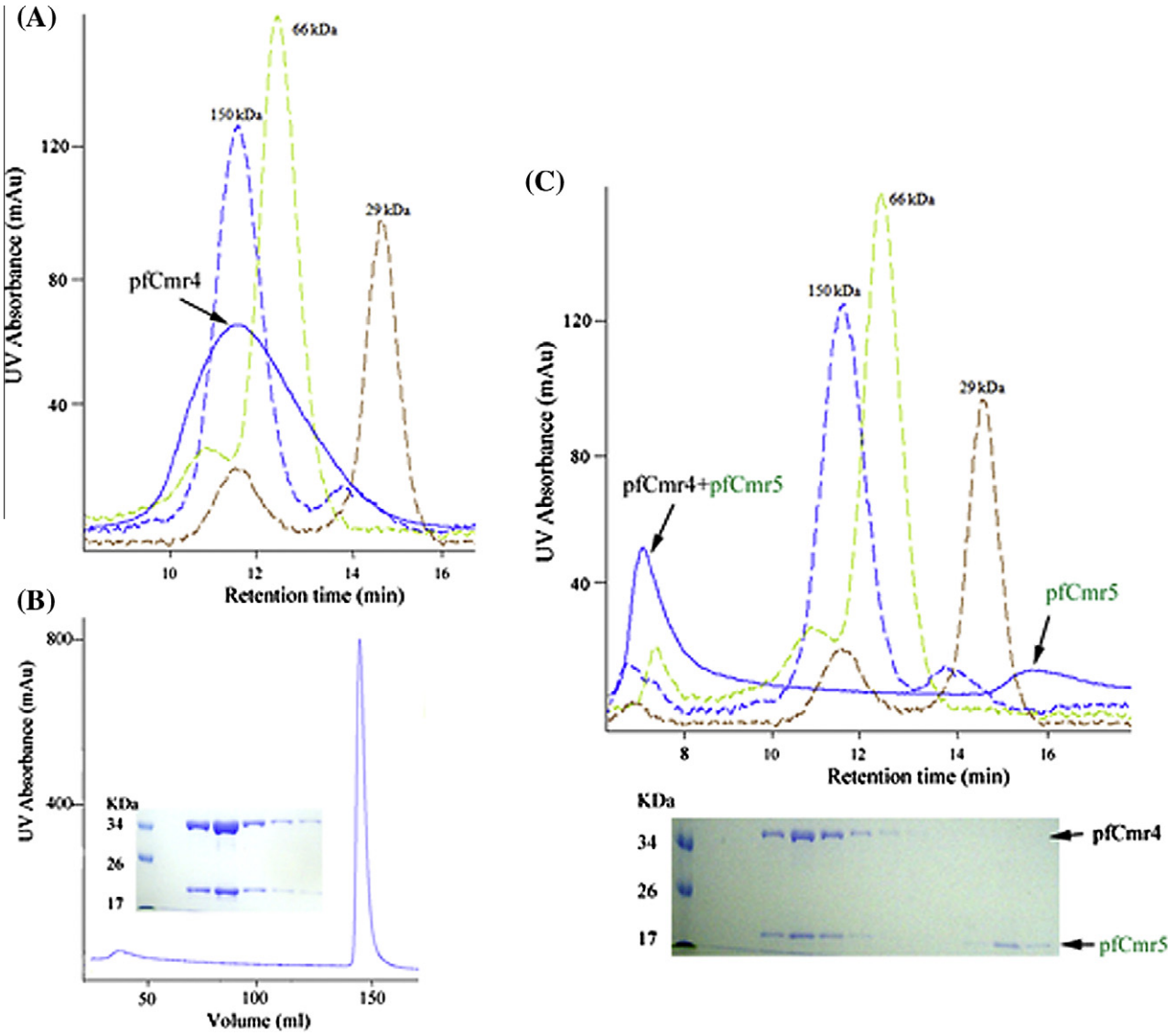

Fig. 4. Interaction of pfCmr5 with pfCmr4. (A) SEC of the purified pfCmr4. The profile for the injected pfCmr5 is drawn with a blue line. (B) Anion exchange chromatography of mixed pfCmr5 and pfCmr4 proteins. Two independently purified proteins were mixed in vitro and bound to the HiTrapQ anion exchange column, which was eluted using a 0–500 mM NaCl gradient and were visualized using Coomassie Blue-stained 10% (w/v) SDS–PAGE. (C) SEC of mixed pfCmr5 and pfCmr4 proteins. The elution profile from the Superose 12 10/300 GL is drawn with a blue line and the eluted fractions were visualized using Coomassie Blue-stained 10% (w/v) SDS–PAGE.

invokes a trimeric structure of ttCmr5 is, if anything, not favorable in pfCmr5 (Fig. 2C). It should also be noted that these hydrophobic residues are not conserved in ssCmr5 and afCmr5 (Fig. 1A), indicating that the difference here may have a critical effect on the oligomerization of Cmr5 proteins.

Similarly in ttCmr5, the polar residues are localized, and charged patches are formed on the pfCmr5 surface (Fig. 3). One positively charged patch is formed at the entrance of the α1-helix by the residues Arg15, Lys16, Arg20, and Arg21 along with Lys141 on the α6-helix. The basic character here might be increased by the disordered, untraced residues Lys11 and Lys12. The Arg151 and Arg152 residues form another small basic patch nearby. In the vicinity of this positively charged patch, there is a negatively charged patch formed by a number of acidic residues, Asp38, Glu73, Asp100, Asp102, and Glu103 on one side and Glu32, Asp35, Glu42, Glu43, and Glu160 on the other side. Interestingly, two basic residues, Lys39 and Lys159, occupy the center of this negatively charged patch. Overall, pfCmr5 and afCmr5 present less electro-potentially polarized and delocalized surfaces than those of ttCmr5, which has positively and negatively charged, localized surfaces, especially around the subunit interfaces at either side of trimeric structure (Fig. 3).

3.3. The pfCmr5 protein interacts with pfCmr4

We performed a number of in vitro assays to detect pfCmr5's biophysical interaction with other pfCmr proteins (Fig. 4). As mentioned in Methods, recombinant proteins of pfCmr5 and pfCmr4 were independently purified and mixed. Subsequently, anion exchange chromatography was carried out, which revealed two proteins of uniform stoichiometry in several fractions (Fig. 4B). The calculated pIs of pfCmr5 and pfCmr4 from their primary sequences are 8.61 and 5.59, respectively. Therefore, the binding of pfCmr5 to and the co-elution of two proteins from the anion exchange column at pH 7.5 strongly indicated the presence of direct interaction between these two proteins.

Next, we performed SEC to further check the interaction between them. A pfCmr4 protein of approximately 33 kDa forms an oligomeric protein in solution (Fig. 4A), although its exact oligomeric states cannot be identified. The SEC analysis of the mixture of pfCmr5 and pfCmr4 exhibited two peaks (Fig. 4C) with two proteins of the same stoichiometry via several fractions at the first peak and only the pfCmr5 at the second peak, which was excessive when compared with pfCmr4 (Fig. 4C). These SEC data strongly suggest that pfCmr5 directly interacts with pfCmr4. In addition, a noticeable interaction with the other pfCmr proteins was not observed in our tested conditions.

4. Concluding remarks

The Cmr5 is one of the widely distributed proteins in organisms that have CRISPR adaptive immune systems including *S. solfataricus*. The elucidated pfCmr5 structure demonstrates the conservation of a common α-helical bundle structure in Cmr5 proteins (Fig. 1B), and its comparison with other Cmr5 structures indicates the presence of structural variations in the intervening region (Fig. 2A). In contrast to the trimeric structure of ttCmr5 (Fig. 2A), pfCmr5 behaves as a monomeric protein both in the crystal and solution (Fig. 2C). Seven non-polar residues that form the oligomeric structure at the subunit interface of the ttCmr5 trimer (Fig. 1A) are not conserved in the structures of pfCmr5 and afCmr5 that form a monomeric structure. These hydrophobic sequences are absent in ssCmr5 (Fig. 1A), indicating that ssCmr5 may exist as a monomeric protein. A highly positively-charged localized surface is formed at ttCmr5, which gives a clue concerning ttCmr5's role as a nucleic acid-binding protein [10]. This surface is partially conserved in the monomeric pfCmr5 and afCmr5. However, its electro-potential is much weaker than that of ttCmr5 (Fig. 3A). Many RAMP-module containing proteins, for example, Cmr proteins, have been known to interact with RNA molecules. Therefore, a RAMP module with a positively charged surface in pfCmr5 implies that Cmr5 may function as an RNA-binding protein, or it might help other Cmr proteins to bind RNA. The dispensability of pfCmr5 in the cleavage function of the recombined Cmr effector complex in *P. furiosus* [8] is suggestive of its eligibility as a member of the effector complex. However, ssCmr5 takes part in forming the Cmr effector complex in *S. solfataricus* [9]. Furthermore, pfCmr5 demonstrated direct interaction in solution with pfCmr4 (Fig. 4) that was critical for the clearance of the add RNAs [8]. Therefore, we suggest that pfCmr5 may influence the effector complex in a yet unsolved way, for example, by affecting the RNA-binding affinity of the Cmr effector complex or the assembly of other Cmr proteins. Nonetheless, the described data here is not enough to clarify the role of pfCmr5. Further work is required for any definitive conclusion that explains the Cmr5 structural features and in vitro results described herein.

Acknowledgments

This work was supported by Basic Science Research Program through the National Research Foundation of Korea funded by the Ministry of Education, Science and Technology of Korea (2010-0008560).

References

[1] Bolotin, A., Quinquis, B., Sorokin, A. and Ehrlich, S.D. (2005) Clustered regularly interspaced short palindrome repeats (CRISPRs) have spacers of extrachromosomal origin. Microbiology 151, 2551–2561.
[2] Mojica, F.J., Diez-Villasenor, C., Garcia-Martinez, J. and Soria, E. (2005) Intervening sequences of regularly spaced prokaryotic repeats derive from foreign genetic elements. J. Mol. Evol. 60, 174–182.
[3] Barrangou, R., Fremaux, C., Deveau, H., Richards, M., Boyaval, P., Moineau, S., Romero, D.A. and Horvath, P. (2007) CRISPR provides acquired resistance against viruses in prokaryotes. Science 315, 1709–1712.
[4] Sorek, R., Kunin, V. and Hugenholtz, P. (2008) CRISPR-a widespread system that provides acquired resistance against phages in bacteria and archaea. Nat. Rev. Microbiol. 6, 181–186.
[5] van der Oost, J., Jore, M.M., Westra, E.R., Lundgren, M. and Brouns, S.J. (2009) CRISPR-based adaptive and heritable immunity in prokaryotes. Trends Biochem. Sci. 34, 401–407.
[6] Brouns, S.J., Jore, M.M., Lundgren, M., Westra, E.R., Slijkhuis, R.J., Snijders, A.P., Dickman, M.J., Makarova, K.S., Koonin, E.V. and van der Oost, J. (2008) Small CRISPR RNAs guide antiviral defense in prokaryotes. Science 321, 960–964.
[7] Marraffini, L.A. and Sontheimer, E.J. (2010) CRISPR interference. RNA-directed adaptive immunity in bacteria and archaea. Nat. Rev. Genet. 11, 181–190.
[8] Hale, C.R., Zhao, P., Olson, S., Duff, M.O., Graveley, B.R., Wells, L., Terns, R.M. and Terns, M.P. (2009) RNA-guided RNA cleavage by a CRISPR RNA–Cas protein complex. Mol. Cell 139, 945–956.
[9] Zhang, J., Rouillon, C., Kerou, M., Reeks, J., Brugger, K., Graham, S., Reimann, J., Cannone, G., Liu, H., Albers, S.V., Naismith, J.H., Spagnolo, L. and White, M.F. (2012) Structure and mechanism of the CMR complex for CRISPR-mediated antiviral immunity. Mol. Cell 45, 303–313.
[10] Sakamoto, K., Agari, Y., Agari, K., Yokoyama, S., Kuramitsu, S. and Shinkai, A. (2009) X-ray crystal structure of a CRISPR-associated RAMP module Cmr5 protein from *Thermus thermophilus* HB8. Proteins 75, 528–532.
[11] Aslanidis, C. and de Jong, P.J. (1990) Ligation-independent cloning of PCR products (LIC-PCR). Nucleic Acids Res. 20, 6069–6074.
[12] Otwinowski, Z. and Minor, W. (1997) Procession of X-ray diffraction data collected in oscillation mode. Methods Enzymol. 276, 307–326.
[13] McCoy, A.J., Grosse-Kunstleve, R.W., Storoni, L.C. and Read, R.J. (2005) Likelihood-enhanced fast translation functions. Acta Crystallogr. D Biol. Crystallogr. 61, 458–464.
[14] Emsley, P. and Cowtan, K. (2004) Coot: model-building tools for molecular graphics. Acta Crystallogr. D Biol. Crystallogr. 60, 2126–2132.
[15] Jones, T.A., Zou, J.Y., Cowan, S.W. and Kjeldgaard, M. (1991) Improved methods for building protein models in electron density maps and the location of errors in these models. Acta Crystallogr. D Biol. Crystallogr. A47, 110–117.
[16] Adams, P.D., Afonine, P.V., Bunkóczi, G., Chen, V.B., Davis, I.W., Echols, N., Headd, J.J., Hung, L.W., Kapral, G.J., Grosse-Kunstleve, R.W., McCoy, A.J., Moriarty, N.W., Oeffner, R., Read, R.J., Richardson, D.C., Richardson, J.S.,

Terwilliger, T.J. and Zwart, P.H. (2007) PHENIX: a comprehensive Python-based system for macromolecular structure solution. Acta Crystallogr. D Biol. Crystallogr. 66, 213–221.

[17] Brünger, A.T., Adams, P.D., Clore, G.M., DeLano, W.L., Gros, P., Grosse-Kunstleve, R.W., Jiang, J.S., Kuszewski, J., Nilges, M., Pannu, N.S., Read, R.J., Rice, L.M., Simonson, T. and Warren, G.L. (1998) Crystallography & NMR system: a new software suite for macromolecular structure determination. Acta Crystallogr. D Biol. Crystallogr. 54, 905–921.

[18] Davis, I.W., Murray, L., Richardson, J.S. and Richardson, D.C. (2004) MolProbity: structure validation and all-atom contact analysis for nucleic acids and their complexes. Nucleic Acids Res. 32, W615–W619.

[19] Larkin, M.A., Blackshields, G., Brown, N.P., Chenna, R., McGettigan, P.A., McWilliam, H., Valentin, F., Wallace, I.M., Wilm, A., Lopez, R., Thompson, J.D., Gibson, T.J. and Higgins, D.G. (2007) Clustal W and Clustal X version 2.0. Bioinformatics 23, 2947–2948.